Supporting Information

Striped Poly(diacetylene) Monolayers Control Adsorption of Polyelectrolytes and Proteins on 2D Materials and Elastomers

Jeremiah O. Bechtold†, Juan C. Arango†, Anni Shi†, Anamika Singh†, Shelley A. Claridge*,†,§

†Department of Chemistry, Purdue University, West Lafayette, IN 47907
§Weldon School of Biomedical Engineering, Purdue University, West Lafayette, IN 47907

*Address correspondence to: claridge@purdue.edu, (phone) 765-494-6070

EXPERIMENTAL METHODS

Materials. Chloroform (≥99.5 % purity), poly(sodium 4-styrenesulfonate) (PSS) ($M_w \approx 1{,}000{,}000$), poly (acrylic acid) (PAA) ($M_w \approx 450{,}000$), and octadecylamine (ODAm, ≥99.0 %), tetrahydrofuran (THF, ≥99.9 %), ammonium hydroxide, lithium aluminum hydride (95 %), and oxalyl chloride (98 %) were purchased from Sigma Aldrich (St. Louis, MO) and used as received. Potassium phosphate (monobasic, ACS grade) was purchased from Research Products International (Mt. Prospect, IL) and used as received. Absolute ethanol was purchased from Decon Laboratories, Inc. (King of Prussia, PA) and used as received. Calcium chloride dihydrate, methanol (≥99.8 %), hexanes (≥98.5 %), sodium sulfate, dichloromethane (DCM, anhydrous ≥99.8 %), N,N-dimethylformamide (DMF), and diethyl ether (≥ 99.7%) were purchased from Fisher Scientific (Hampton, NH) and used as received. Albumin from bovine serum (BSA) tetramethylrhodamine conjugate was purchased from Thermo Fisher Scientific (Hillsboro, OR) and used as received. 1,2-Bis(10,12-tricosadiynoyl)-*sn*-glycero-3-phosphoethanolamine (dPE, >99.0 % purity) was purchased from Avanti Polar Lipids (Alabaster, AL) and used as received. For transfer to polydimethylsiloxane (PDMS), SYLGARD 184 silicone elastomer kits containing base and curing (crosslinking) agent were purchased from Dow Chemical Company (Midland, MI). 10,12-Pentacosadiynoic acid (PCDA, ≥ 97.0% purity) and 10,12-tricosadiynoic acid (TCDA, ≥ 98.0% purity) were purchased from Sigma-Aldrich (St. Louis, MO), dissolved in chloroform, and filtered using a 13-mm syringe filter with a PTFE membrane and 0.2-µm pores (VWR, Radnor, PA). Ultrahigh purity nitrogen (UHP N_2, 99.999 % purity) was purchased from Indiana Oxygen Company (Indianapolis, IN). Lipids were deposited on 1 cm × 1 cm highly oriented pyrolytic graphite (HOPG, MicroMasch, Watsonville, CA) substrates. Substrates were cleaved immediately prior to sample deposition. All initial steps in the transfer process were carried out under UV-filtered light to prevent unwanted polymerization. PELCO conductive liquid silver paint, standard SEM pin stub mounts, AFM specimen discs (alloy 430), PELCO Formvar/carbon 400 mesh TEM grids, and double-coated carbon conductive tape were purchased from Ted Pella, Inc. (Redding, CA). Milli-Q water (≥18.2 MΩ · cm resistivity) was used whenever water was required in an experiment.

General procedure for the synthesis of a 10,12-diynamine from a 10,12-diynoic acid. 10,12-Pentacosadiynamine (PCD-NH_2) and 10,12-tricosadiynamine (TCD-NH_2) were prepared from a 10,12-diynoic acid (*i.e.,* 10,12-pentacosadiynoic acid (PCDA) and 10,12-tricosadiynoic acid (TCDA), respectively) using a modification of previously reported literature procedures,[1, 2] described briefly here. First, 10,12-diynoic acid (1 eq) was dissolved in anhydrous DCM under N_2 atmosphere. Oxalyl chloride (1.3 eq) and DMF (N, N-dimethylformamide) (2 drops) were added to the solution. The reaction mixture was stirred at room temperature overnight and concentrated under reduced pressure to obtain 10,12-diynoyl chloride as a yellow oil which was used for the next step without further purification. Next, in a round-bottom flask, 28–30 % aqueous ammonium hydroxide (1.3 eq) was added. 10,12-Diynoyl chloride (1 eq) was dissolved in THF and the resulting solution was added to the ammonium hydroxide solution at 0 ˚C. The reaction mixture was stirred at room temperature for 6 h. The product was extracted with DCM (3 × 50 mL) and the combined organic extract was dried over anhydrous Na_2SO_4. The DCM was evaporated under reduced pressure to yield 10,12-diynoyl amide as a white solid. 10,12-Diynoyl amide (1 eq) was placed in a round-bottom flask. Anhydrous diethyl ether was added to the flask under N_2 atmosphere, yielding a white suspension. Subsequently, $LiAlH_4$ (10 eq) was added to the suspension at 0 ˚C and the reaction mixture was stirred at room temperature for 20 h. After the reaction was complete, the mixture was cooled to 0 ˚C and treated with sequential dropwise addition of water, aqueous NaOH (15 % *w*/*w*) and water. The mixture was filtered to remove inorganic impurities, and the filtrate was dried over anhydrous Na_2SO_4. After drying over Na_2SO_4, the solvent was evaporated under reduced pressure to yield the final product (10,12-diynamine). PCD-NH_2 and TCD-NH_2 were dissolved in chloroform and filtered using a 13-mm syringe filter with a PTFE membrane and 0.2-µm pores (VWR, Radnor, PA) prior to use.

Langmuir-Schaefer transfer. Unless otherwise stated in the manuscript, monolayers of TCD-NH_2, PCD-NH_2, ODAm, and dPE were prepared *via* a temperature-controlled Langmuir-Schaefer conversion process we have reported previously, that utilizes a custom-built temperature-controlled transfer stage.[3] The stage was utilized in conjunction with a MicroTrough XL Langmuir–Blodgett trough. HOPG substrates mounted on a standard 12-mm diameter stainless-steel AFM specimen disc were mounted on a magnet recessed in the temperature-controlled stage. Conductive carbon tape was used to affix the HOPG to the specimen disk surface to ensure temperature uniformity was achieved across the substrate surface. The temperature of the substrate was measured using a thermocouple prior to dipping.

TCD-NH_2 and PCD-NH_2 films were created at the air–water interface by depositing 36 µL of 0.75 mg/mL chloroform solution on a subphase comprised of 40 mM $CaCl_2$ in Milli-Q water, maintained at 30 °C. Following deposition, 15 min was allowed for the chloroform to evaporate. Barriers were then swept inward at 6.23 mm/min to achieve the target mean molecular area (*e.g.,* 30 Å^2/chain); the feedback mechanism was subsequently switched to maintain the surface pressure measured at the point at which the target mean molecular area was achieved. HOPG substrates were freshly cleaved, mounted on the thermally controlled stage, and heated to 70 °C, then lowered (at 2 mm/min) into contact with the subphase. Contact was maintained for 2 min. The HOPG was then lifted out of contact at a rate of 2 mm/min.

ODAm films were created at the air–water interface by depositing 18 µL of 0.5 mg/mL chloroform solution on a subphase of 40 mM $CaCl_2$ maintained at 30 °C. Following deposition, 15 min was allowed for the chloroform to evaporate. Trough barriers were then moved inward at 3.0 mm/min, until the target mean molecular area of 30 Å^2/chain was achieved, and subsequently switched to maintain the surface pressure measured when the setpoint mean molecular area (30 Å^2/chain) was originally achieved. HOPG substrates were freshly cleaved, mounted on the thermally controlled stage, and heated to 35 °C, then lowered (at 2 mm/min) into contact with the subphase. Contact was maintained for 2 min. The HOPG was then lifted out of contact at 2 mm/min.

dPE films were created at the air–water interface by depositing 36 µL of 0.6 mg/mL chloroform solution on a subphase of Milli-Q water maintained at 30 °C. Following deposition, 15 min was allowed for the chloroform to evaporate. Trough barriers were then moved inward at 6.23 mm/min, until a target surface pressure of 30 mN/m was achieved. HOPG substrates were freshly cleaved, mounted on the thermally

controlled stage, and heated to 50 °C, then lowered (at 2 mm/min) into contact with the subphase. Contact was maintained for 2 min. The HOPG was then lifted out of contact at 2 mm/min.

After contact with the subphase was broken, HOPG substrates was blown dry with UHP N_2. Finally, unless otherwise stated in the manuscript, HOPG substrates were placed under a hand-held UV lamp (254 nm, 8 W) for 1 h with ~2 cm between the lamp and the substrate to induce diyne photopolymerization.

AFM imaging. All AFM measurements were performed using a Bruker (Bruker Instruments, Billerica, MA) MultiMode AFM, equipped with an E scanner, under ambient conditions utilizing Bruker RFESP-75 tips (nominal force constant 3 N/m and radius of curvature <10 nm). Micrographs were collected in tapping mode.

Image analysis. Images were processed using ImageJ analysis software and Gwyddion scanning probe microscopy data visualization and analysis software to preform plane flattening, median line corrections, scar artifact removal, contrast adjustment and pixel counting. Adsorbed polymer mass was estimated by digital image analysis within ImageJ after the raw bitmap files were processed by mean plane subtraction, median row alignment, and horizontal scar correction using Gwyddion. The pixels/nm scale was calibrated for individual micrographs then the pixels representing polymers in the micrograph were manually highlighted and contour lengths measured to generate a polymer length in nm. At least 3 images were analyzed for each data point graphed. For BSA adsorption experiments, histograms of pixel intensities were compiled using ImageJ, first converting each image into an RGB stack, and utilizing intensities from the red channel, to select for fluorescence emission from the BSA-TRITC conjugates.

SEM imaging. SEM imaging of microcontact printed dPE square arrays under high magnification was performed using a Teneo VS SEM (FEI Company, Hillsboro Oregon) at a working distance of ~ 7 mm using the segmented in-lens T3 secondary electron (SE) detector. For best resolution, image acquisition beam currents of 0.10–0.8 nA were typically utilized with a 32-µm diameter aperture at an accelerating voltage of 5 kV. Substrates were mounted with conductive carbon tape to standard SEM pin stub specimen mounts where a small amount of colloidal silver paint (PELCO®, Ted Pella, Inc.) was applied along the perimeter of the HOPG to enhance substrate-mount conductivity.

Molecular Modeling. Software packages Maestro and Macromodel (Schrödinger, Cambridge, MA) were used respectively to visualize molecular structures and to perform force field minimizations. Energy minimizations on all models was performed using OPLS_2005 force field, with extended cutoffs for van der Waals, electrostatic, and hydrogen-bonding interactions. Minimizations were performed using the Polak–Ribiere conjugate gradient (PRCG) algorithm and gradient method with 50 000 runs and a convergence threshold of 0.05.

Contact angle titrations. Contact angle titrations were performed using an Attension Theta optical tensiometer (Biolin Scientific, Espoo, Finland). Buffers with 20 mM buffering capacity at a range of pH values from 2 to 12 were purchased from Sigma-Aldrich and used as received. For each measurement, on both HOPG and PDMS substrates, a 3 µL droplet of buffer was applied to the substrate. The angle between the substrate and the line tangent to the droplet surface was calculated by the tensiometer within 10 s of deposition, and recorded as the advancing contact angle. Subsequently, the buffer droplet was withdrawn, using a syringe with a 32-gauge needle, until the solvent front on the substrate receded; this value was recorded as the receding angle. Each contact angle graphed is the average of 27 data points distributed across 3 substrates from 3 sample sets. Typically, 9 measurements were recorded from each 1 × 1 cm substrate.

Preparation of PDMS stamps. Stamps were prepared using a modification of published procedure,[4] described briefly here. SYLGARD 184 silicone elastomer base and curing (crosslinking) agent were combined at a 10:1 *m*/*m* ratio, and thoroughly mixed. Formvar-and-carbon-coated copper 400 mesh TEM grids were placed, Formvar side down, in a glass Petri dish. The PDMS mixture was poured over the TEM grids, then deaerated in a vacuum desiccator until no bubbles remained. The PDMS was cured for 24 h at 60 °C; the TEM grids were then gently peeled from the PDMS, generating a micropatterned surface. Micropatterned stamps were cleaned by sonication in a 1:1:1 (*v*/*v*/*v*) mixture of ethanol, methanol, and Milli-Q water for 60 min, and subsequently placed in an oven for 1 h at 60 °C to allow residual polar solvent mixture to evaporate. The micropatterned stamps were then soaked in hexanes for 6 h, replacing the solvent with fresh hexanes every 2 h. Finally, the micropatterned stamps were dried for 24 h at 60 °C and then stored covered in a petri dish, pattern side up, prior to use.

Microcontact printing of dPE. Inking and printing steps were performed following a previously published procedure,[5] described briefly here. The molecular ink solution was prepared at 2.5 mg/mL in $CHCl_3$ and diluted to 0.4 mg/mL with ethanol. Prior to inking, the PDMS stamp was rinsed with ethanol and blown dry with ultra-high purity (UHP) N_2. The stamp was then immersed for 1 min in the ink solution, removed and blown dry with UHP N_2, and placed pattern side up at room temperature for 1 h. The pattern side of the PDMS stamp was brought into contact with a freshly cleaved HOPG substrate for 1 min and carefully lifted off the surface. The microcontact printed HOPG substrate was then exposed to UV, to induce diyne photopolymerization, for 1 h under a held UV lamp (254 nm, 8 W) for 1 h with ~2 cm between the lamp and substrate surface.

Covalent transfer of PDA striped phase from HOPG to PDMS. The covalent transfer of striped PDA monolayers from HOPG to PDMS was performed using a previously published procedure,[6] described briefly here. SYLGARD 184 silicone elastomer base and curing (crosslinking) agent were combined at a 10:1 (mass/mass) ratio. After thorough mixing (5 min), PDMS was poured onto a HOPG substrate functionalized with a polymerized polydiacetylene amphiphile film. The PDMS mixture was deaerated in a vacuum desiccator to remove all air bubbles, then cured for 24 h at 60 °C. Cured PDMS was carefully peeled away from the HOPG substrate, exfoliating the PDA monolayer onto the PDMS surface.

Wide-field fluorescence microscopy. Wide-field fluorescence micrographs were obtained using an Olympus BX-51 optical microscope with an Olympus DP71 color camera. Images were acquired using either a 40X (metallographic, plan-fluorite aberration correction, NA = 0.75, infinity corrected optics) or a 100X (metallographic, apochromatic and flat field correction, NA = 0.95) brightfield objective. A UMWB2 filter cube was utilized (460–490 nm excitation band-pass filter, dichroic filter wavelength of 500 nm, long-pass emission filter wavelength of 520 nm). Typical dwell times for imaging ranged from 1/1.5 to 5 s with a resolution of 1024 × 1024 pixels.

Confocal fluorescence microscopy and spectral imaging. Confocal micrographs and associated spectra were acquired utilizing a Zeiss LSM 880, Axio Examiner upright confocal microscope. Unless otherwise stated, excitation was provided by a 488-nm Ar laser set to 100 % power. Data were obtained using a 20X objective (plan-apochromatic, dry, NA = 0.80), with a 0.17-mm cover glass placed on the sample, and a 32-channel GaAsP spectral photomultiplier tube detector. Micrographs and corresponding spectra were obtained at a resolution of 2856 × 718 pixels, a bit depth of 8 bits, a dwell time of 11.75 µs/pixel (using unidirectional scanning and averaging 16 times per line), and a pinhole set to 1 Airy unit. For detection, 23 of the 32 channels were used to collect data, with bins centered at values from 495–691 nm and a resolution (bin width) of 8.9 nm. Monolayer spectra were corrected to remove a peak centered at 513 nm resulting from PDMS emission.

Polyelectrolyte deposition. Polyelectrolyte solutions were prepared in Milli-Q water at concentrations of 4 µg/mL for PSS and 2 µg/mL for PAA (~25 µM in the polyelectrolyte repeat unit, in each case).

Spin-coating tests of polyelectrolyte adsorption were performed utilizing an SPS Polos SPIN 150i Spin-coater. In each test, a substrate was mounted in the spincoater, and 20 µL of Milli-Q water was deposited on the substrate. After 15 s, the Milli-Q water droplet was spin coated on the substrate by rotating the spin-coater stage with an acceleration of 400 rpm/s to a final velocity of 2400 rpm/s, which was maintained for 30 s. Subsequently, 20 µL of the polyelectrolyte solution to be tested was deposited on the substrate. After 5 s, the polyelectrolyte solution droplet was spin coated onto the substrate, using the same conditions described above. Substrates were then stored under ambient conditions until characterization.

For dip-coating tests of polyelectrolyte adsorption, each substrate was lowered into contact with the polyelectrolyte solution, at a slight angle, and contact was maintained for 30 s. The substrate was then lifted out of contact with the polyelectrolyte solution, dried with UHP N_2, and stored under ambient conditions.

To deposit high-coverage coatings of PSS, substrates were lowered into contact with a 1 mg/mL PSS solution in Milli-Q water, retained in the PSS solution for 10 min, then removed from the solution and blown dry with UHP N_2. Substrates were subsequently washed twice with Milli-Q water for 5 min, and blown dry with UHP N_2 between washings. This PSS dipping process was then repeated, and the substrates stored under ambient conditions.

BSA deposition. Solutions of bovine serum albumin tetramethylrhodamine conjugate (TRITC–BSA) were prepared at 0.5 mg/mL in 20 mM potassium phosphate in Milli-Q water, adjusted to pH 3.0, 5.0, or 7.0 using HCl or NaOH. Solution pH was verified just prior to experiment. Functionalized and unfunctionalized PDMS substrates were prepared, cut to a 0.5 cm × 0.5 cm area per substrate, and placed on a glass slide. A 0.1 mL droplet of the TRITC–BSA solution was deposited on each substrate. PDMS substrates were then covered and incubated under a Petri dish for 10 min. The droplets of TRITC–BSA were removed from the surfaces; substrates were subsequently washed with a 10 mM potassium phosphate solution and with Milli-Q water for 30 s to remove weakly-adsorbed material, and then blown dry with UHP N_2.

Larger AFM and SEM images illustrating LS assembly of striped phase films of PCD-NH_2, ODAm, TCD-NH_2, and dPC on HOPG

In the main manuscript, Figure 2 shows AFM and SEM images illustrating the lamellar and domain structure for striped polydiacetylene (PDA) films. Here, we show larger AFM and SEM images (Figure S1 and S2), illustrating nanoscale and microscale molecular ordering achieved using thermally regulated Langmuir-Schaefer (LS) conversion. In Figure S1, AFM images of (a) PCD-NH_2, (b) ODAm, (c) TCD-NH_2, and (d) dPC exhibit striped phase domains with edge lengths > 100 nm. Also visible in the images are long linear features generally crossing the entire image from left to right, which correspond to HOPG step edges (an example is labeled in Figure S1b).

In Figure S2, SEM images provide a microscale view of PCD-NH_2 striped phase assembly on HOPG. Long linear defects evolve in ordered monolayers during polymerization (Figure S2, left), due to restructuring as diacetylenes rehybridize to form the PDA backbone. In SEM images, the orientation of such defects can be used to infer molecular row orientation. Thus, long-range orientation of cracking defects is indicative of long-range ordering in the monolayer (here, up to scales >20 μm). In other experiments, we utilize conditions that result in rounded or oval microscopic vacancies in the monolayer (Figure S2, right), visible as darker regions in the SEM image. Such vacancies provide contrast useful in verifying transfer to PDMS via fluorescence microscopy.

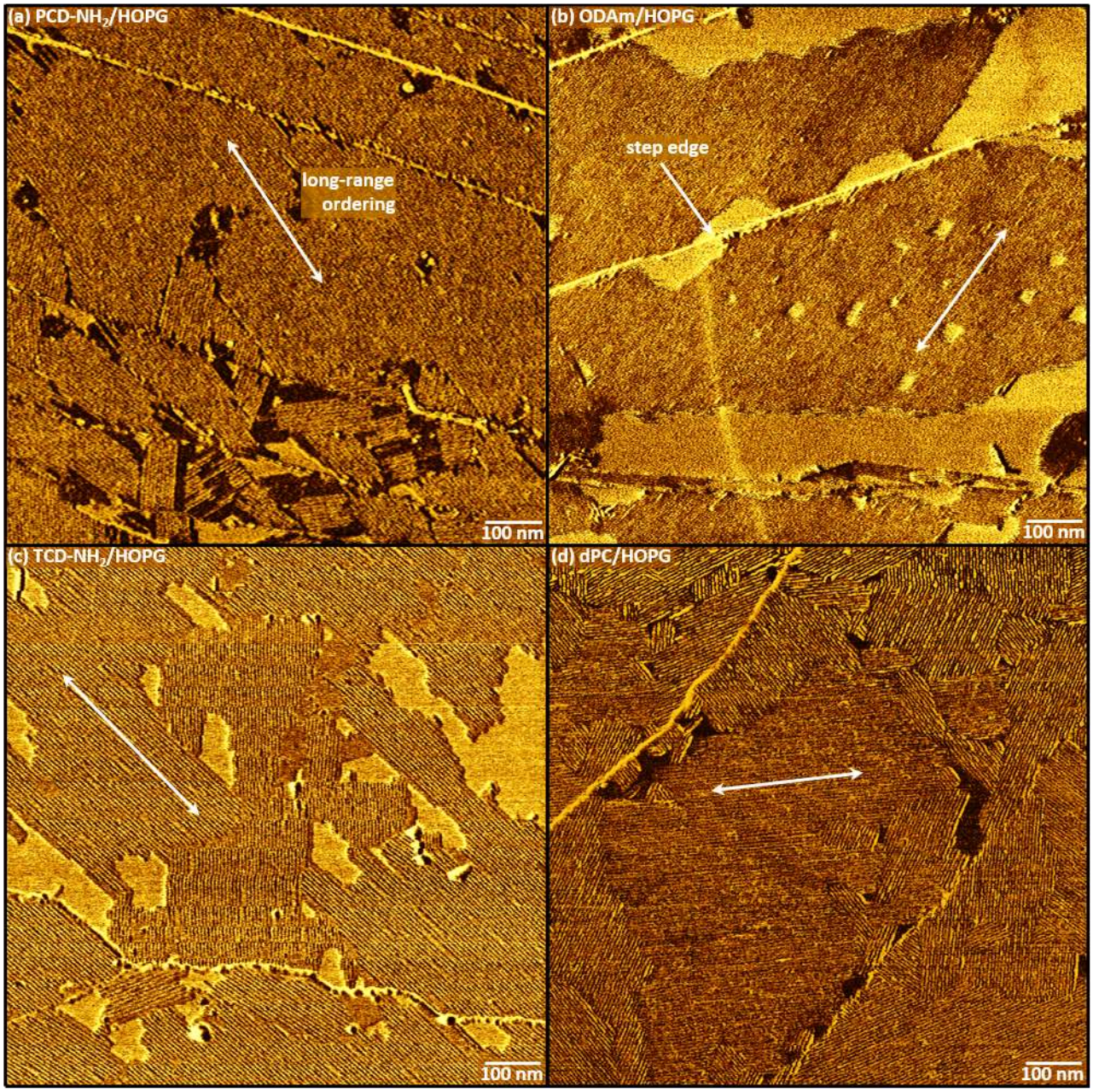

Figure S1. AFM micrographs illustrating nanoscale lamellar ordering in striped domains of (a) PCD-NH_2, (b) ODAm, (c) TCD-NH_2, and (d) dPC on HOPG.

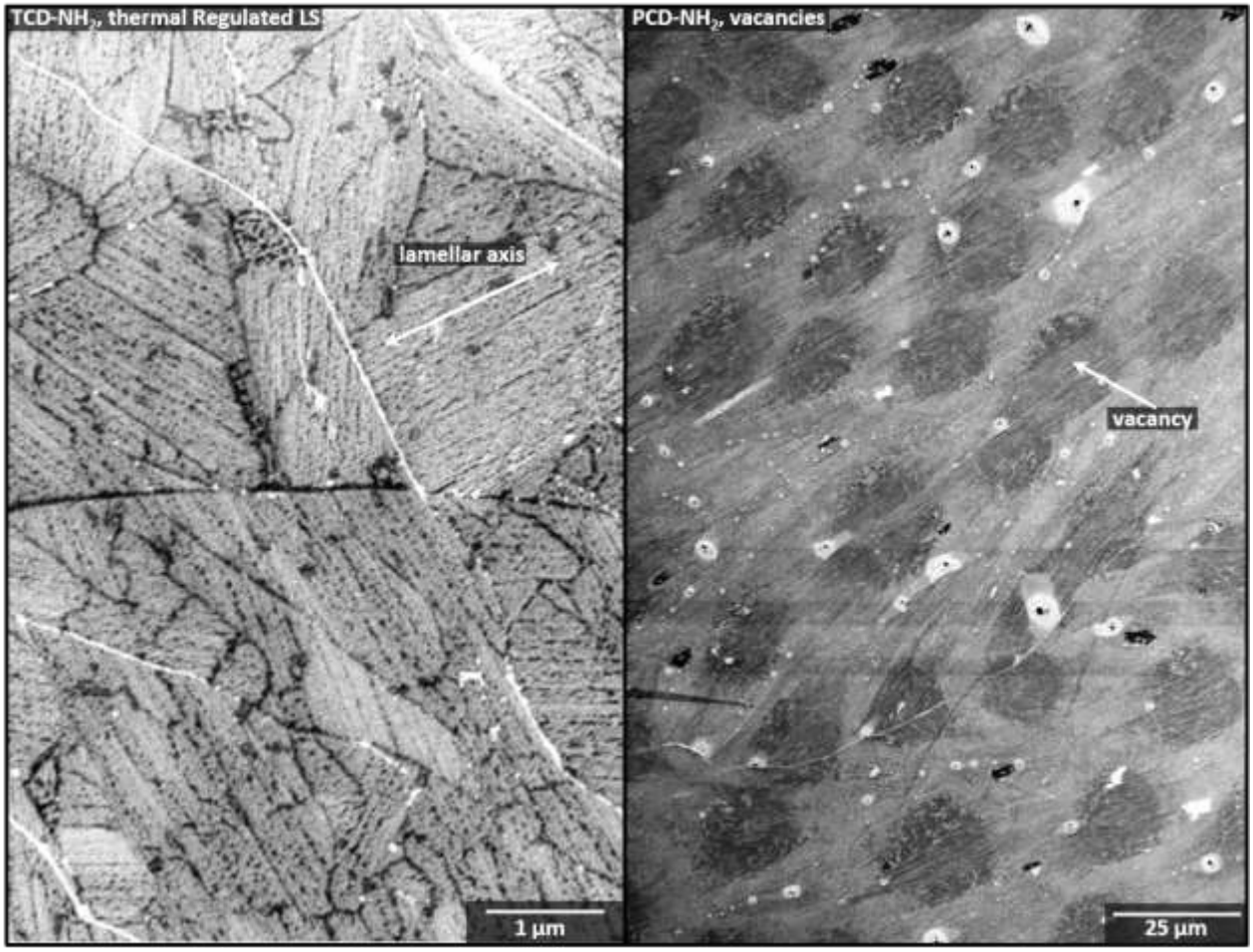

Figure S2 SEM images of PCD-NH_2 illustrating (a) long-range ordering of striped phase domains and (b) microscopic oval vacancies produced by selected LS conditions.

Larger AFM micrographs illustrating adsorption of polyelectrolytes

In the manuscript, Figure 3 contains AFM micrographs of polyelectrolyte adsorption on striped phases of PCD-NH_2 and ODAm. Here, we show larger AFM micrographs of striped phase domains with PSS deposited via spin coating or dip coating. Micrographs of spin-coated PSS on PCD-NH_2 (Figure S3a) and ODAm (Figure S3c) illustrate differences in PSS ordering, possibly consistent with reordering of ODAm monolayers during PSS adsorption. Micrographs of dip-coated PSS on PCD-NH_2 (Figure S3b) and ODAm (Figure S3d) illustrate shorter PSS segmental lengths in both cases (in comparison with spin-coating), which may indicate that solvent flow during spin-coating is in part responsible for more extended conformations adopted by the PSS. Vacancies are also observed in monolayers on dip-coated substrates, particularly in monomeric ODAm monolayers.

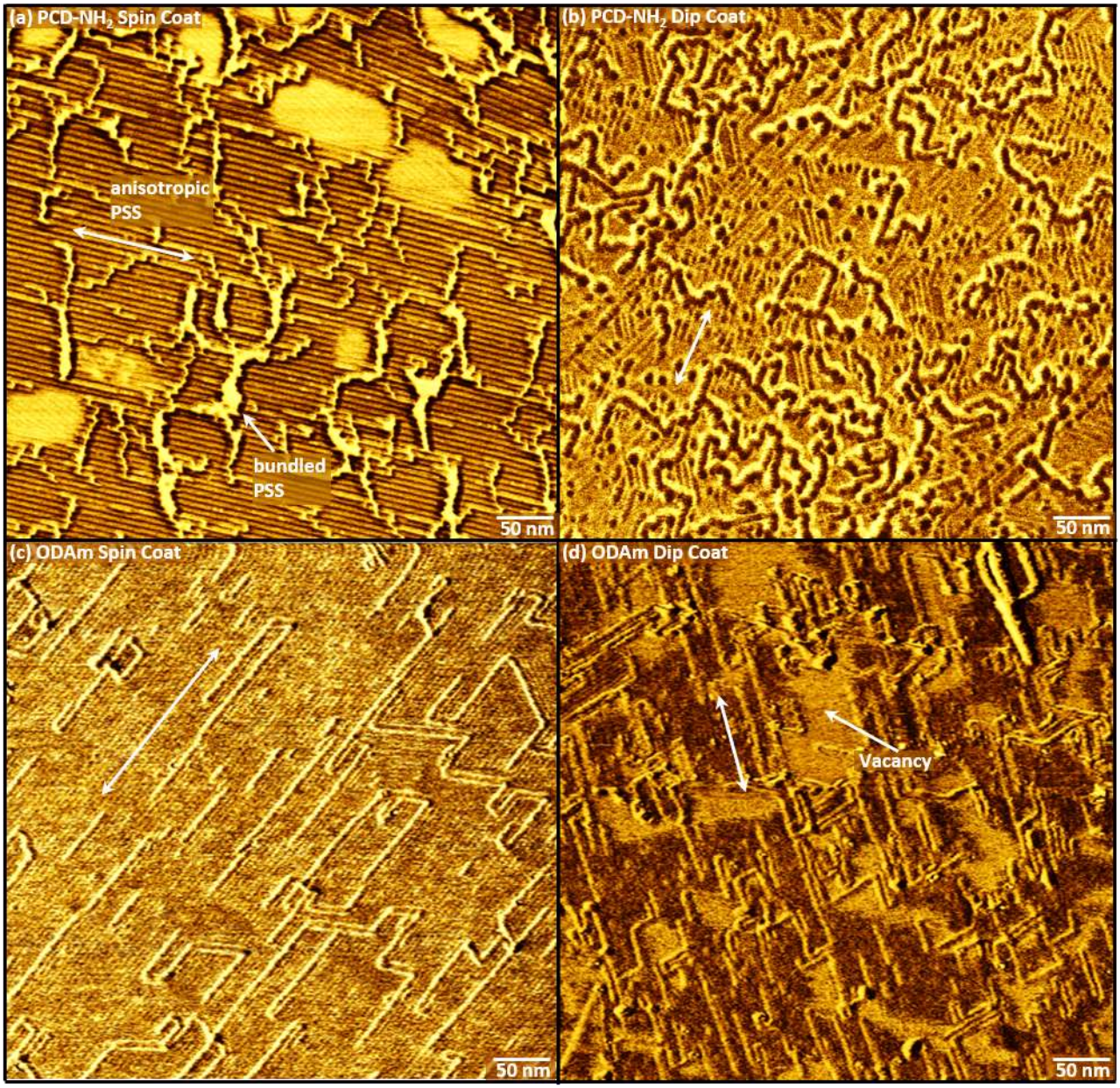

Figure S3. AFM micrographs illustrating the anisotropic adsorption of PSS in epitaxy with ordered rows of (a,b) PCD-NH_2 and (c,d) ODAm. Dip coated samples (b,d) illustrate monolayer disordering and desorption cause from PSS solution exposure.

Morphologies of PSS adsorbed on bare HOPG (Figure S4) are different than those shown above. Figures S4a shows the bare HOPG surface with step edges visible across the micrograph. Spin coating PSS on bare HOPG results in small aggregates and minimal polyelectrolyte adsorption to the surface (Figure S4b). Dip coating produced bundles of PSS adjacent to step edges (Figure S4c).

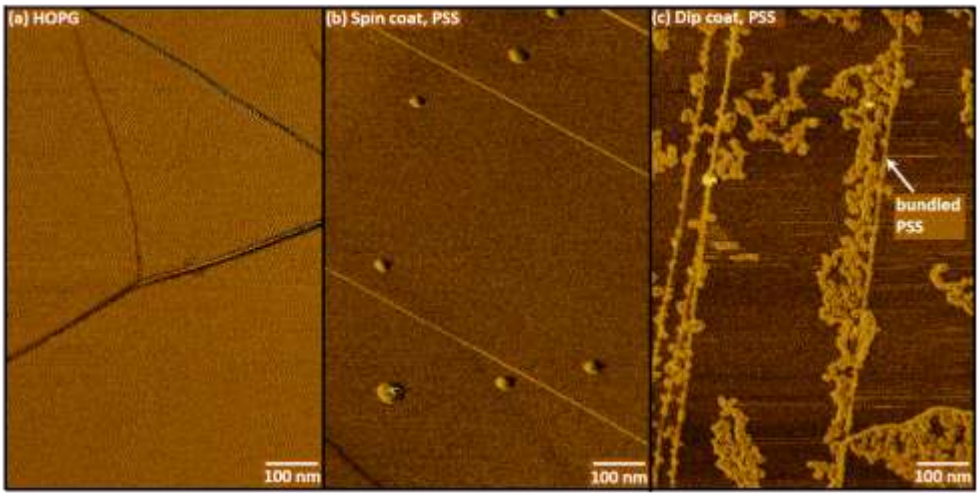

Figure S4. AFM micrographs of (a) bare HOPG and HOPG after exposure to PSS through (b) spin-coating or (c) dip-coating.

In Figure 5 of the main manuscript, we illustrated polyelectrolyte adsorption on functionalized PDMS. Figures S5-7 show larger-scale AFM micrographs of surfaces illustrated in the main manuscript, as well as substrates not exposed to PSS or PAA. Figure S5a shows bare PDMS without exposure to polyelectrolyte. To ensure topographical consistency between the control and functionalized samples, for bare PDMS controls, the 10:1 base:crosslinker PDMS mixture was cured in contact with a bare HOPG substrate. Figure S5b shows an AFM micrograph of bare PDMS dip-coated using the same procedures used to generate the TCD-NH_2 functionalized PDMS (TCD-NH_2/PDMS+PSS) shown in Figure 6 of the manuscript. Unlike the extensive PSS adsorption shown in Figure 6, we observe minimal PSS adsorption on the bare PDMS surface after 2 min of exposure. Figure S5c shows PDMS functionalized with TCD-NH_2, without exposure to polyelectrolytes. We note that for single-chain amphiphiles such as TCD-NH_2, linear features are only very faintly visible against the pore structure of the PDMS, whereas features are typically somewhat more clear for dual-chain amphiphiles such as dPE, as shown in the main manuscript. We believe this may relate to the long polymerization lengths (~100 nm) necessary to create visible linear features in AFM images, while polymerization lengths >10 nm are adequate to achieve multiple anchor points on the PDMS mesh. Overall, imaging the soft, porous PDMS surface at high resolution is quite challenging relative to HOPG, and SEM imaging is not feasible on the nonconductive PDMS substrate, so typically transfer is verified based on fluorescence microscopy and spectroscopy, as illustrated in the main manuscript.

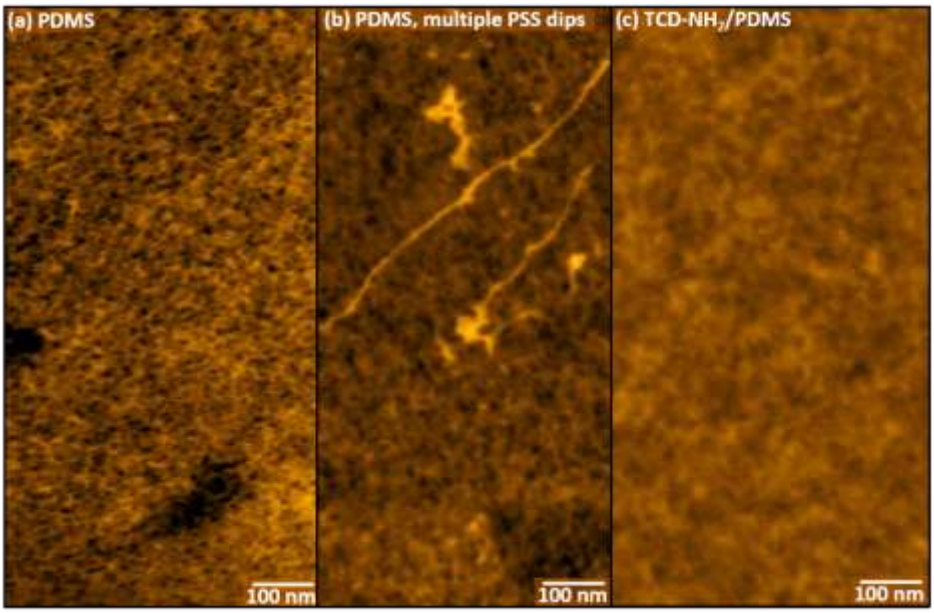

Figure S5. AFM micrographs of example controls: (a) bare PDMS, (b) bare PDMS exposed to multiple rounds of PSS dip-coating, (c) PDMS functionalized with TCD-NH_2.

In the manuscript, we demonstrated polyelectrolyte adsorption on functionalized PDMS in Figure 5. Here we provide enlarged AFM micrographs of substrates illustrating PAA (Figure S6) and PSS (Figure S7) adsorption.

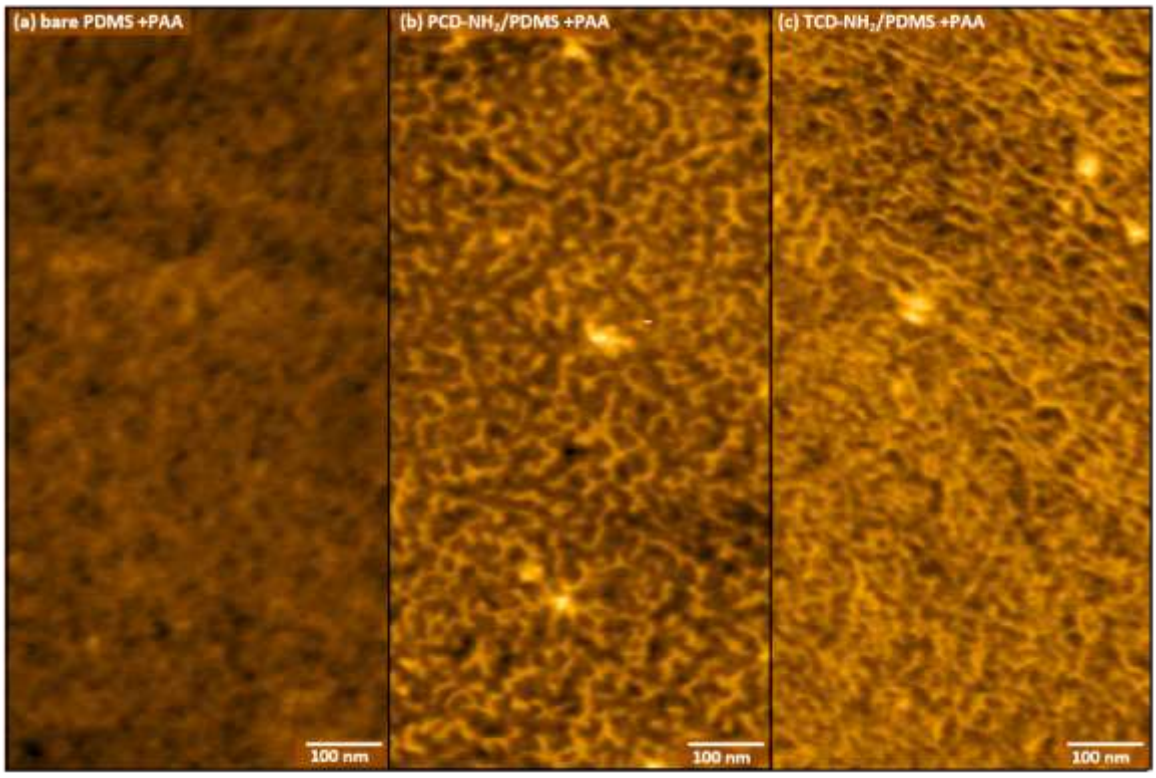

Figure S6. AFM micrographs of substrates dip-coated with PAA: (a) bare PDMS, (b) PCD-NH_2/PDMS, and (c) TCD-NH_2/PDMS.

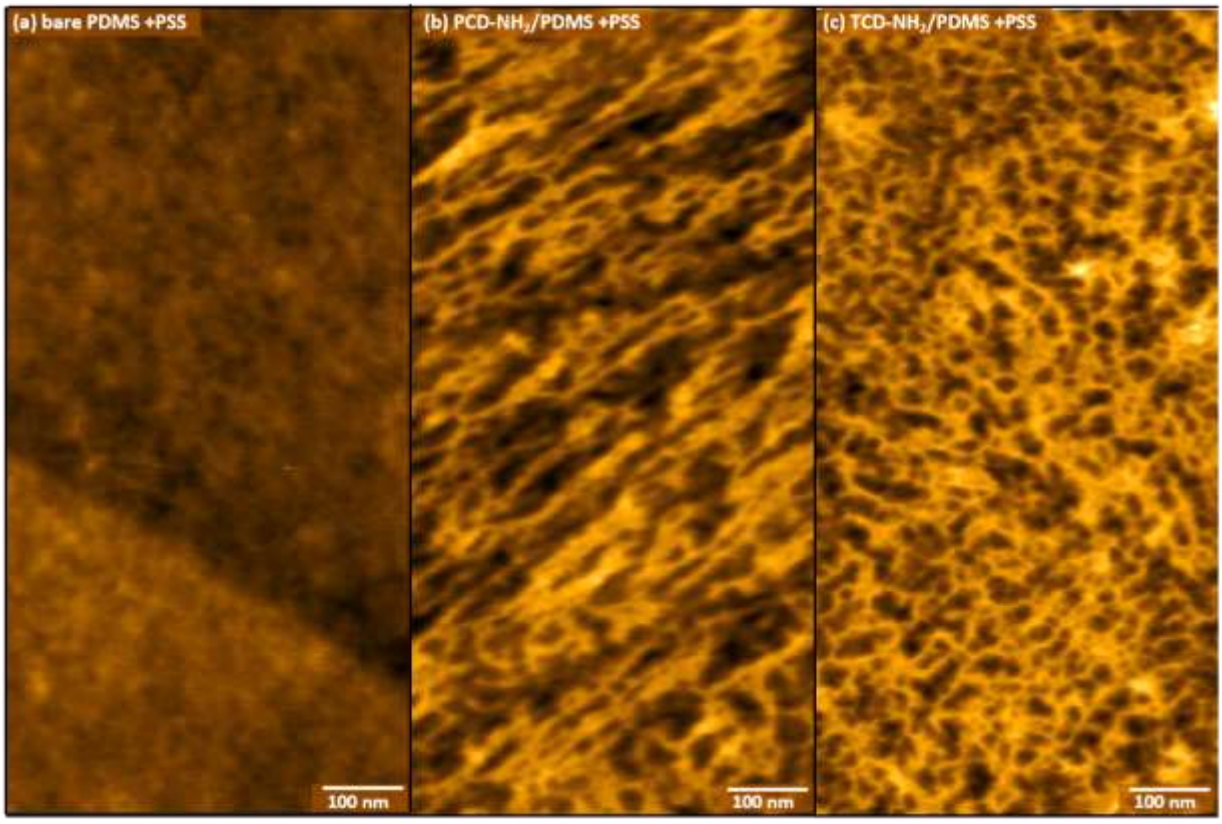

Figure S7. AFM micrographs of substrates dip-coated with PSS: (a) bare PDMS, (b) PCD-NH_2/PDMS, and (c) TCD-NH_2/PDMS.

Larger SEM and fluorescence images illustrating the transfer of striped PDA films to PDMS.

In the experiments described in the main manuscript, we carried out PDMS transfer using striped phase monolayers with a set of chemistries and morphologies designed to impact surface adsorption of polyelectrolytes. Here, we show enlarged SEM and fluorescence images of the monolayer morphologies. For TCD-NH_2 transfer, we first assembled monolayers on HOPG using LS conversion conditions that generate oval vacancies, to facilitate characterization *via* fluorescence microscopy following transfer to PDMS. SEM images (Figure S8a) illustrate oval vacancies (darker regions) in a monolayer on HOPG (similar to the smaller image shown in Figure 2). Following transfer of TCD-NH_2 and PCD-NH_2 films to PDMS, fluorescence images (Figure S8b,c) also contain oval vacancies (lower-fluorescence regions).

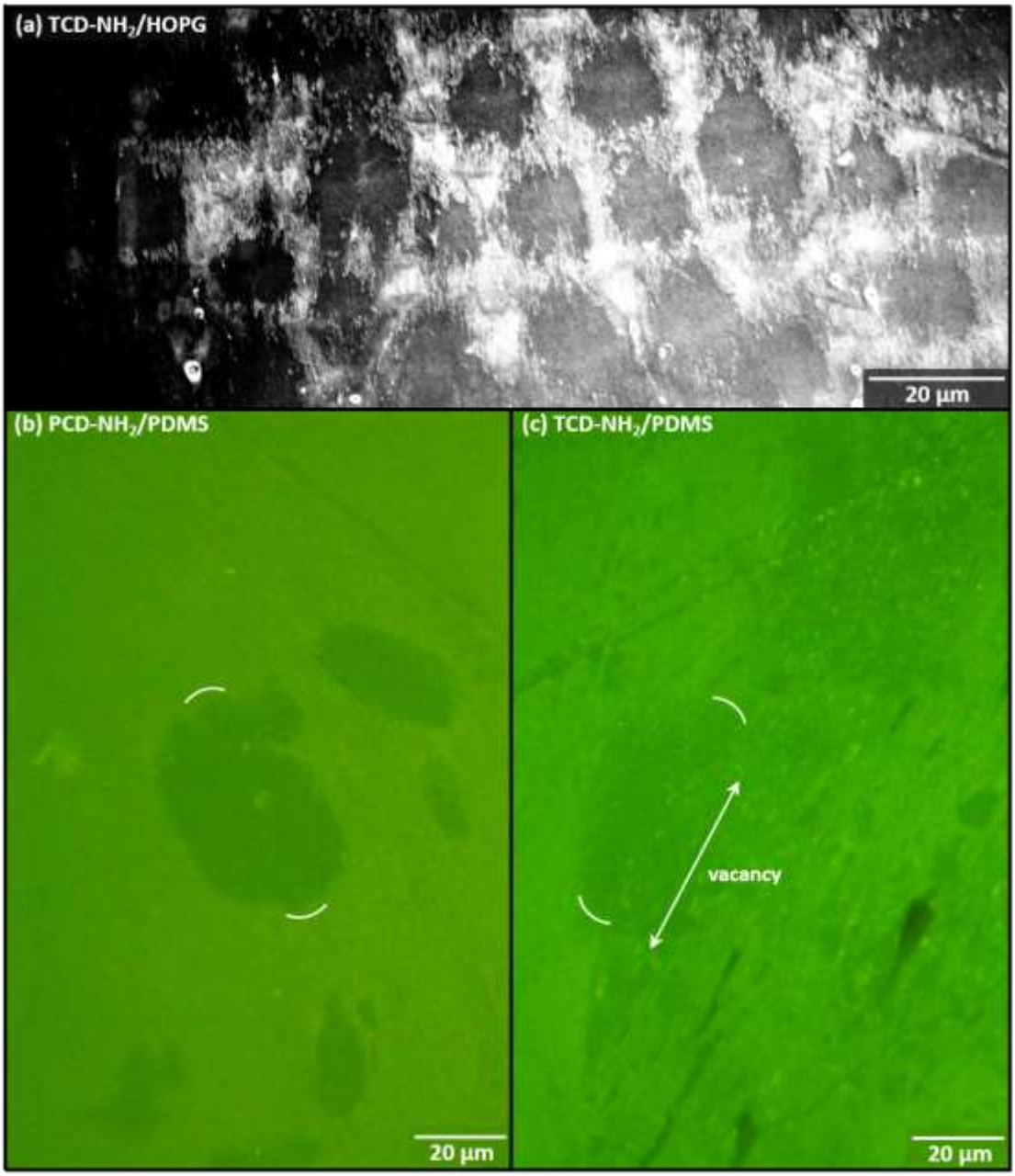

Figure S8. SEM and fluorescence images illustrating congruence of PCD-NH_2 and TCD-NH_2 vacancy domain structure before and after transfer to PDMS. SEM image of vacancies in (a) TCD-NH_2/HOPG. Fluorescence images of vacancies within (b) PCD-NH_2/PDMS and (c) TCD-NH_2/PDMS.

Figure S9 shows filtered fluorescence emission images and spectra for functionalized and unfunctionalized PDMS. In the wavelength range from 495–700 nm, TCD-NH_2/PDMS (Figure S9a) exhibits stronger green fluorescence emission, in areas morphologically similar to striped PDA domains, in comparison with bare PDMS (Figure S9b), which presents a uniform background. Spectra from these two classes of substrates (Figure S9c) illustrate the stronger emission from TCD-NH_2/PDMS, in the wavelength range associated with PDA emission (blue trace), in comparison with the dPE striped phases (gold trace), which we have reported in more detail previously[6]. Spectral images at wavelengths >520 nm (Figure S9d–f), in the wavelength range associated with TRITC–BSA emission, all three classes of substrates (TCD-NH2/PDMS (Figure S9d), TCD-NH2/PDMS+PSS (Figure S9e), and bare PDMS (Figure S9f)) appear uniformly dark.

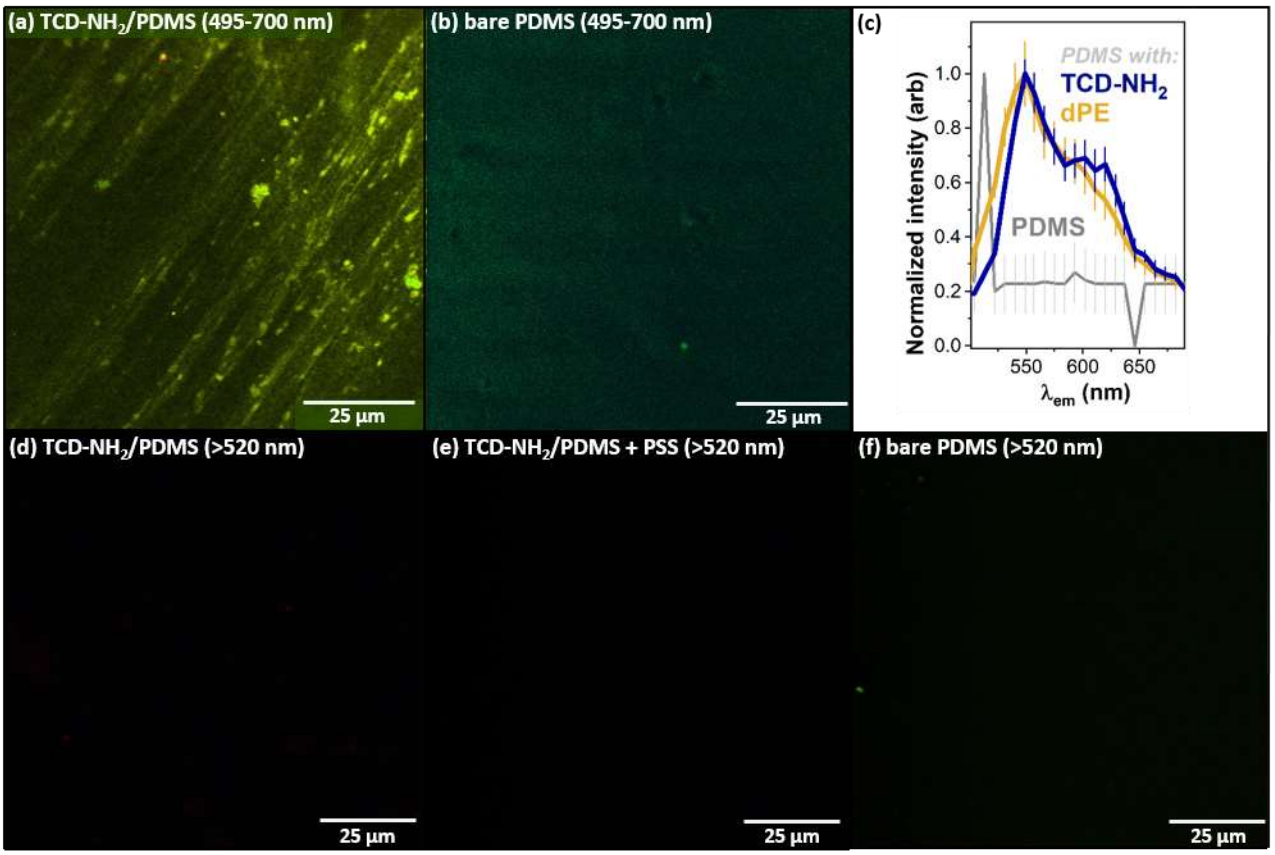

Figure S9. Fluorescence images and spectra of functionalized and unfunctionalized PDMS. (a) TCD-NH_2/PDMS and (b) bare PDMS and (c) spectra of fluorescence emission at wavelengths from 495-700 nm. (d–f) Images of fluorescence emission at wavelengths >520 nm (relevant to BSA emission) for (d) TCD-NH_2/PDMS, (e) TCD-NH_2/PDMS+PSS, and (f) bare PDMS, all prior to exposure to TRITC–BSA.

In the BSA adsorption experiments in the main manuscript, we generate surfaces with square patterns of dPE phospholipids on PDMS. The squares are generated by microcontact printing dPE on HOPG as described in the experimental section, and subsequently transferred to PDMS through the PDMS curing process described in the experimental section. The process we use generates squares in which the regions near the edges are comprised of dPE striped phases. In the center, there is a region of standing phase dPE, with a low-density region between the standing and striped regions (presumably depleted as the standing phase is generated). Square patterns of the phospholipid on HOPG are clearly visible in SEM images (Figure S10a). However, the large scale of the squares (50 µm) and the relatively small topographic heights of the features (3 nm for standing phase, and ~0.5 nm for striped phase) mean that although the squares are visible in AFM phase images (Figure S10b), variations in the height of the HOPG substrate make it difficult to view patterns directly by height (compare Figures S10c and d, height and phase images of the same area, showing a circular area near the center of a square). A line scan taken across Figure S10c (white line in lower center) reveals an ~70 nm total height change across that area of the substrate (total image width 40 µm). If polynomial background subtraction is used on similar images (Figure S10f), line scans (Figure S10g) illustrate an ~3 nm height change at the edge of the center circular areas, consistent with a feature that is predominantly standing phase, although there may be regions of multilayer distributed throughout the circle center.

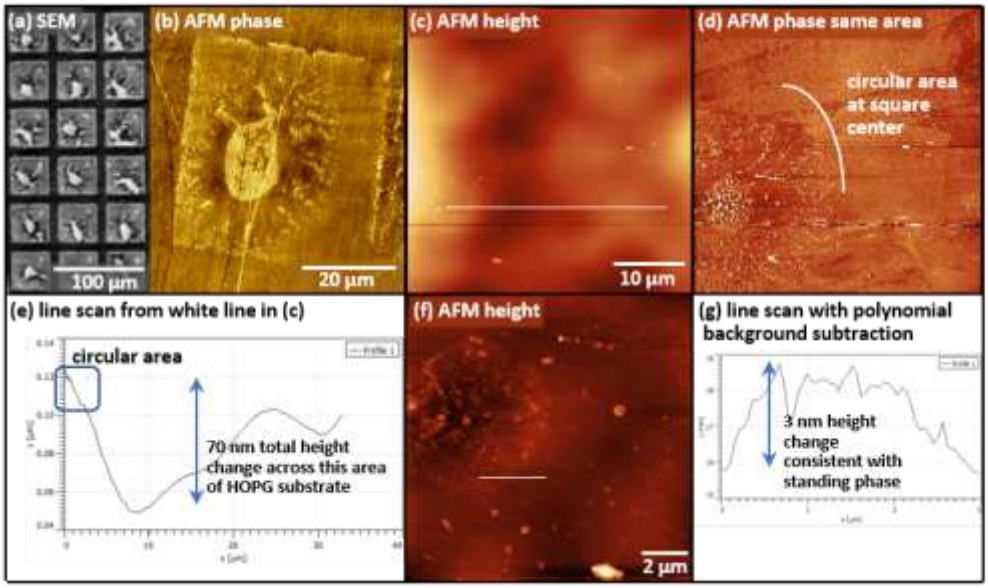

Figure S10. (a) SEM image of µCP dPE on HOPG. (b–d) AFM images of square patterns on HOPG: (b) large-scale AFM phase, (c) smaller-scale AFM height, showing substantial variations in background topography that make line profiles challenging, (d) AFM phase image in same area, showing a circular area at the center of a patterned square. (e) Line scan acquired at white line across (c), illustrating large variations in surface topography. (f) AFM height image of a circular center with polynomial background substraction and (g) line profile taken near edge of circle, illustrating topographical changes consistent with standing phase near center of square.

Fluorescence imaging of TRITC-BSA adsorption to functionalized and unfunctionalized PDMS.

In Figure S11, we show fluorescence images of representative PDMS substrates after TRITC-BSA adsorption. Each image panel is 100 μm x 100 μm.

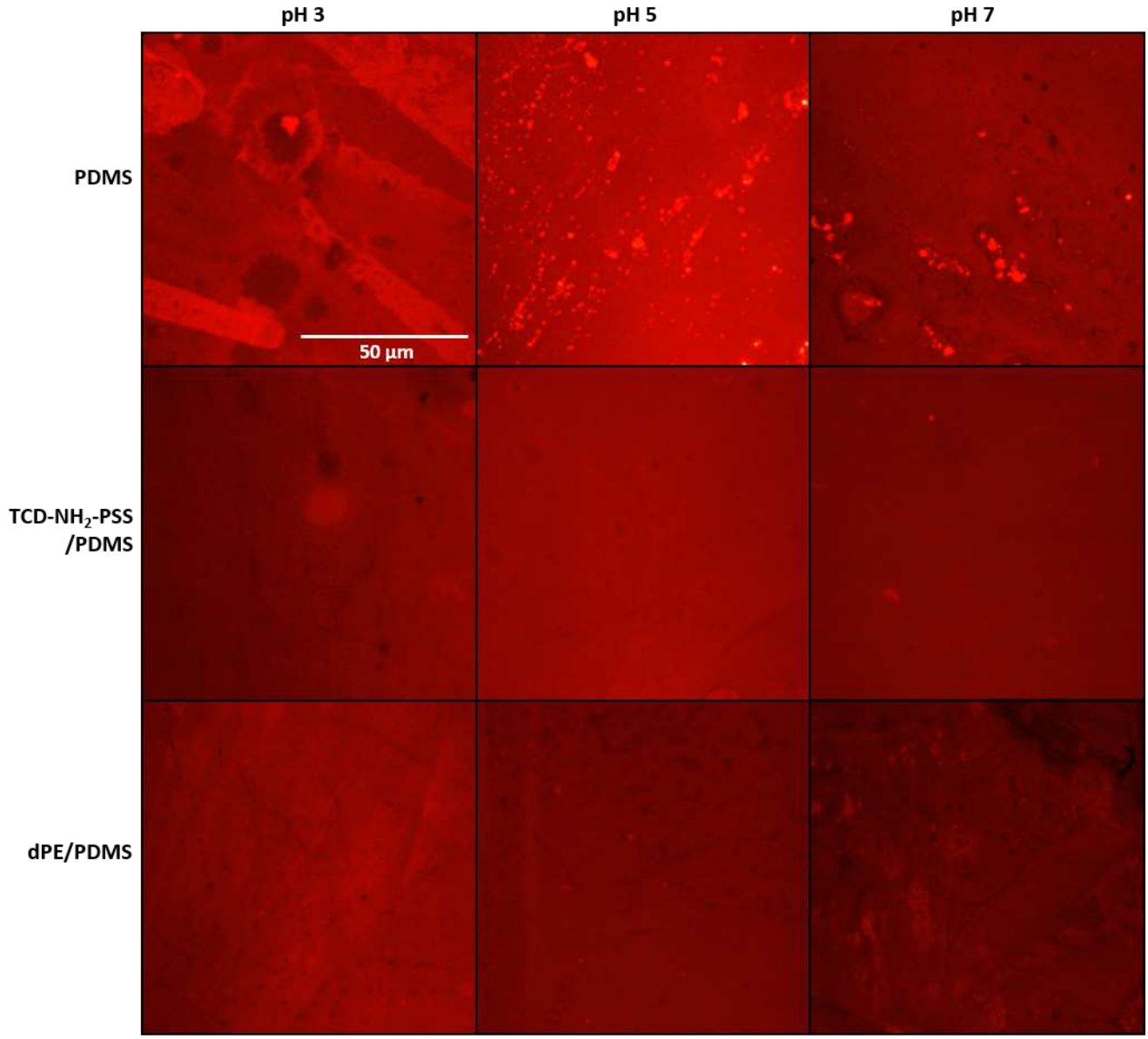

Figure S11. Fluorescence images of TRITC-BSA adsorption on: bare PDMS (top row), and PDMS functionalized with TCD-NH_2 +PSS (middle row), and μCP dPE (bottom row).

REFERENCES

1. Howarth, N. M.; Lindsell, W. E.; Murray, E.; Preston, P. N., Lipophilic peptide nucleic acids containing a 1,3-diyne function: synthesis, characterization and production of derived polydiacetylene liposomes. *Tetrahedron* **2005,** *61*, 8875-8887.

2. Lee, J. P.; Hwang, H.; Chae, S.; Kim, J.-M., A reversibly mechanochromic conjugated polymer. *Chem. Commun.* **2019,** *55*, 9395-9398.

3. Hayes, T. R.; Bang, J. J.; Davis, T. C.; Peterson, C. F.; McMillan, D. G.; Claridge, S. A., Multimicrometer Noncovalent Monolayer Domains on Layered Materials through Thermally Controlled Langmuir-Schaefer Conversion for Noncovalent 2D Functionalization. *ACS Appl. Mater. Interf.* **2017,** *9* (41), 36409-36416.

4. Thakar, R.; Baker, L. A., Lithography-free production of stamps for microcontact printing of arrays. *Anal. Meth.* **2010,** *2*, 1180-1183.

5. Davis, T. C.; Bechtold, J. O.; Hayes, T. R.; Villarreal, T. A.; Claridge, S. A., Hierarchically Patterned Striped Phases of Phospholipids: Toward Controlled Presentation of Carbohydrates. *Faraday Discuss.* **2019,** *219*, 229-243.

6. Davis, T. C.; Bechtold, J. O.; Shi, A.; Lang, E. N.; Singh, A.; Claridge, S. A., One Nanometer Wide Functional Patterns with a Sub-10 Nanometer Pitch Transferred to an Amorphous Elastomeric Material. *ACS Nano* **2021,** *15*, 1426-1435.